A Miniaturized Antenna with Optimum Q-Factor and High NFD for UWB Microwave Imaging

M. Tarikul Islam, M. Samsuzzaman, I. Yahya, and M. T. Islam

Center of Advanced Electronic and Communication Engineering
Faculty of Engineering and Built Environment, Universiti Kebangsaan Malaysia, 43600, Bangi, Malaysia
p94299@siswa.ukm.edu.my, samsuzzaman@ukm.edu.my, iskandar.yahya@ukm.edu.my, tariqul@ukm.edu.my

Abstract **–** This paper presents an ultra-wideband (UWB) micro-strip patch antenna design for microwave breast phantom imaging system. By optimizing the shape of radiating elements, the antenna achieves UWB characteristics with excellent frequency ratio. The antenna was fabricated and tested in both time and frequency domain analysis. Sufficient agreement between the simulated and measured data was observed. The antenna achieves a wider bandwidth of 8.2 GHz (2.5 GHz to 11.2 GHz) with good gain and radiation pattern. The antenna has optimum design comparing to the theoretical Q-factor and the near field directivity (NFD) is also observed. Effective near-field microwave breast phantom measurement systems with an array of 9 UWB antennas is proposed and the performance is tested with and without tumor cells inside the breast phantom. The backward scattered signals analysis shows that the presence of tumor with higher dielectric constant than normal cells. Thus, the proposed antenna can be a good candidate for microwave breast tumor detection.

Index Terms **–** Antenna array, backscattering, microwave breast imaging, NFD, UWB antenna.

I. INTRODUCTION

In recent years, breast cancer is considered an emerging cause of disease of millions of women across the globe with high mortality rate. Only the early detection of this disease is critical to lessen the mortality rate. Currently, X-ray mammography, magnetic resonance imaging (MRI) and ultrasound imaging are used for breast cancer detection. X-ray is the most widespread techniques for screening but it has some major drawbacks including false negative rate higher than 34%, costly and harmful high frequency radiation. [1]. Furthermore, for getting higher resolution image, mammography causes unpleasant breast compression. As a result, research is being conducted to find an alternate method for early efficient detection of breast tumor cell which will be low cost, easy to implement, high positive rate and comfortable for the patient. Human breast is constructed in the comparatively modest model rather than other body parts such as thorax, limbs and abdomen. Remarkably, there is an identical difference between the dielectric properties of normal and malignant breast tissue. This difference of electrical properties related to conductivity and permittivity is the fact that normal breast tissue propagates the microwave signal fluently in a lossy and fatty medium rather than lesions which hold more liquid in the response of blood and water. So, any unwanted cell cluster, or cyst, can be identified in this from the scattered signals. Microwave imaging can be the suitable alternative to the conventional breast tumor detection system with respect to harmless, low cost and high-resolution imaging.

The main aim of the microwave imaging technique is to develop a reliable low-cost imaging system which will be adaptable to clinical applications. After the declaration of the unsilenced band of 3.1–10.6 GHz as ultra-wideband (UWB) frequency by FCC, researchers from academia and industry focus on the various application of this band including several wireless communications, microwave imaging, positioning and tracking etc. UWB antennas can be a good candidate for microwave imaging for its wider bandwidth, good gain and large data transmission rate. So, to get high-resolution images the use of UWB antennas are desirable. Several antennas have been reported in detection for breast tumor cells such as monopole antenna, slot antenna, array antenna, bow-tie antenna, line-fed printed wide-slot antenna, disk shape antenna and planner patch antenna [2-12]. Every antenna has their own characteristics and benefits. The antenna proposed in [2] has narrow bandwidth of 4-8GHz where lower frequency can penetrate the human tissue compared to higher frequencies. The antenna operates in 6 and 12.5 GHz [4] and has a larger dimension compared with the proposed antenna. Similarly the proposed prototype has larger bandwidth comparing to [7, 13]. The proposed design is compact in size compared to [4, 7] and has omnidirectional radiation pattern and higher gain. Most of the reported antennas put emphasis on frequency domain characteristics except [7], where time domain characteristics of the proposed antenna is also

Submitted On: April 30, 2018
Accepted On: August 11, 2018

1054-4887 © ACES

analyzed which is essential for microwave imaging. Again, several array structures of breast imaging systems were also proposed [2, 4, 13]. However, it is still a challenge to develop compact low profile low-frequency antennas which cover a wider bandwidth.

In this paper, a compact UWB antenna is proposed which has excellent frequency ratio and wider bandwidth. The antenna covers the entire UWB band with the operating bandwidth of 3-11.5 GHz. The antenna performance is experimentally verified after fabrication and the main aim was to make this antenna suitable for microwave imaging application. The novel structure of the antenna then used to construct an array setup of 9 antennas surrounding a breast phantom. A near-field imaging system is implemented, and the scattered signals are analyzed to observe the difference between the behavior of the received signals with and without the tumor cells inside the phantom.

II. IMAGING SYSTEM SETUP

A. Miniaturized UWB antenna design and parametric study

For efficient radar imaging system, a compact UWB antenna is desirable that will be efficient in transmitting and receiving signal with minimal frequency dispersion. For this purpose, a compact, low profile, wider bandwidth and high efficient antenna is suitable. The prototype presented in this work has modified shaped radiating element with a dimension of 44 × 42 × 1.5 mm^3. For this dimension, the resonance frequency, in general, can be calculated using the below equation:

$$f_r = \frac{c}{\left[x\sqrt{2(\varepsilon_r+1)}\right]}. \quad (1)$$

Where *fr* is the center frequency, the speed of light is c, ε_r denotes relative permittivity and overall length of the main resonator is x. The dimension is optimized such a way that it can radiate efficiently with large bandwidth spectrum. A modified slotted antenna is generated from a rectangular microstrip patch antenna. The simplest model is the transmission line model that delivers a good physical perception. So this method is mostly accepted for designing the proposed antenna. The antenna coves two radiating element connected with the transmission line W_1. The nonhomogenous line is consists of two dielectric, one is substrate and another one is sorrounding air. The patch radiator dimension is calculated by the simplified formulation of the transmission line model. The width is calculated by:

$$W = \frac{c}{2f_r}\left(\frac{\varepsilon_r+1}{2}\right)^{-\frac{1}{2}}. \quad (2)$$

Here, c is the speed of light in free space and f_r is the resonant frequency. To find the effective permittivity of the substrate the equation can be derived as:

$$\varepsilon_{re} = \frac{\varepsilon_r+1}{2} + \frac{\varepsilon_r-1}{2}\left(1+\frac{12h}{W}\right)^{-\frac{1}{2}}. \quad (3)$$

Here, h is the substrate thickness. The path length (L) can be calculated as:

$$L = \frac{c}{2f_r\sqrt{\varepsilon_{re}}} - 2\Delta L. \quad (4)$$

The design structure of the proposed antenna prototype is shown in Fig. 1. For ensuring a good penetration inside the breast phantom the antenna is optimized for achieving a wider bandwidth including low and high frequency. A modified slotted patch and the partial ground are acting as a main radiating element and the prototype is fed with a transmission line of 50Ω using SMA connector. Several parametric studies during the design of the proposed antenna were done using HFSS simulation solver. Figure 2 illustrates the different tested patch shape. Figure 3 shows the effect of patch shape of the proposed prototype on reflection coefficient (S_{11}). A narrow vertical slot with inside the left arm perturbs the distinctive current flow and density. This modification helps to move the resonant frequency to the lower frequency than the elliptical patch shape. The repetition of the same type of arm structure on the right side helps the upper resonant frequency to shift towards a higher frequency that enhances the bandwidth. Different tested ground shape is shown in Figs. 4 (a-c). The effect of ground shape over the reflection coefficient (S_{11}) is shown in Fig. 4 (d). For investigation, different types and lengths of ground has been preferred to find the best-suited ground shape of the proposed antenna. There is the noticeable effect of bandwidth along with reflection coefficient with respect to the change of ground plane. It seems that the partial ground case has better impedance matching in parametric study but from Fig. 4 (e) it is clear that due to modified proposed ground shape the gain performance is better than the partial ground. According to the electromagnetic wave propagation basic theory of patch antenna, the surface current in the radiating component creates an equal and opposite phase surface current on the ground plane [14]. The compact ground plane creates low cross-coupling effect and aids substantially larger bandwidth. After the numerical analysis, it is observed the proposed partially slotted ground plane covering the non-radiating portion of the feed line offers the widest bandwidth comparing to the other tested shapes.

The simulated current distribution of the proposed antenna on two different frequencies is presented in Fig. 5. At a lower frequency of 4.5 GHz, it is observed that majority of the current concentration is along with feed line and slot of the left portion of the patch and ground slot on the other arm upper portion of the patch conduct a poor amount of current. This indicates that the slot in patch and ground has a significant effect on lower

frequency. So, for lower frequency, the impedance matching is much dependent on modified left slot of the patch and partial slot on ground. For the higher frequency, most of the current concentrate on feedline, knitting of the feedline and upper radiator and upper right slot of the radiator, hence the ground has weak current flow near feed line. Consequently, the ground is weaker than the lower frequency. Also, feed gap has a great impact on impedance matching. Different modified parameters of the proposed antenna are presented in Table 1.

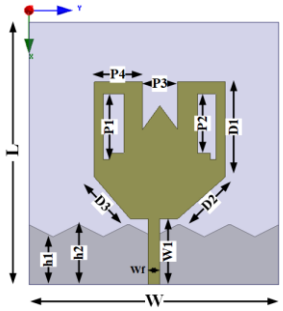

Fig. 1. Antenna geometry.

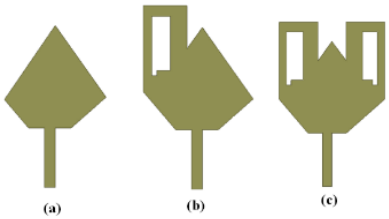

Fig. 2. Different tested patch shapes: (a) without arm, (b) with one arm, and (c) the proposed one.

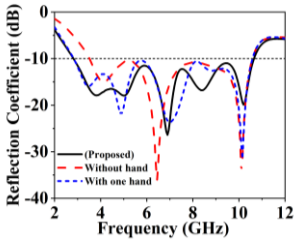

Fig. 3. Reflection coefficient (S_{11}) characteristics of the designed antenna for different patch shape.

The simulated current distribution of the proposed antenna on two different frequencies is presented in Fig. 5. At a lower frequency of 4.5 GHz, it is observed that majority of the current concentration is along with feed line and slot of the left portion of the patch and ground slot on the other arm upper portion of the patch conduct a poor amount of current. This indicates that the slot in patch and ground has a significant effect on lower frequency. So, for lower frequency, the impedance matching is much dependent on modified left slot of the patch and partial slot on ground. For the higher frequency, most of the current concentrate on feedline, knitting of the feedline and upper radiator and upper right slot of the radiator, hence the ground has weak current flow near feed line. Consequently, the ground is weaker than the lower frequency. Also, feed gap has a great impact on impedance matching. Different modified parameters of the proposed antenna are presented in Table 1.

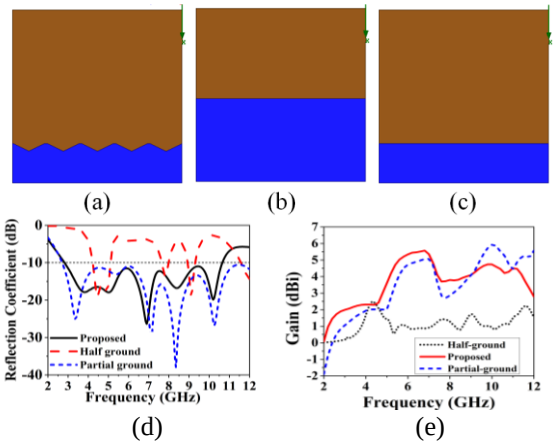

Fig. 4. Different tested ground shapes: (a) proposed, (b) half ground, (c) the partial ground, (d) effect of ground shape on reflection coefficient (S_{11}), and (e) effect of ground shape on peak realized gain.

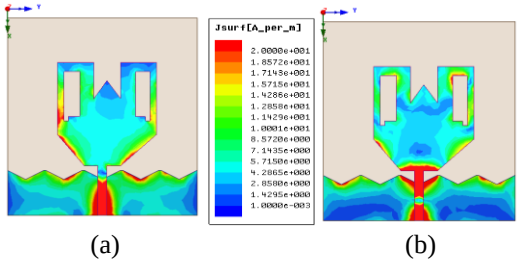

Fig. 5. Surface current distribution at a lower frequency: (a) 4.5 GHz and higher frequency of (b) 8.5 GHz.

Table 1: Modified parameters

Parameters	mm	Parameters	mm
W	42	*P3*	8.1
L	42	*P4*	4.94
D1	16	*h1*	8
D2	10.63	*h2*	10
D3	9.21	*W1*	11
P1	11	*h*	1.6
P2	10		

B. Synthetic and experimental results

The performance of the proposed design is analyzed by EM simulator ANSYS HFSS. HFSS is based on a Finite Element Method (FEM). After the optimization, a prototype is fabricated for experimental verification, as depicted in Figs. 6 (a), (b). A vector network analyzer from Keysight Technologies is used to measure the VSWR responses. The VSWR curves of the optimized design are displayed in Fig. 7. It is evident from the figure that the fabricated design achieved a band from 2.50 GHz to 11 GHz for VSW ≤ 2 which makes it suitable for WiMAX, WLAN, UWB, C-band and X-band communication applications. The slight deviation of the measured VSWR observed at around 6 - 7 GHz band may be due to the mismatch at that band resulted from imperfect prototyping, the effect of feeding cable during measurement and high losses of FR4 dielectric material. StarLab near-field antenna measurement system as shown in Fig. 6 (d) is used to measure the radiation pattern, efficiency and gain of the prototype. Figure 7 (a) represents the measured and simulated voltage standing wave ratio (VSWR) of the proposed prototype from 2GHz - 11GHz. It is observed that a wide bandwidth from 2.5 GHz to 11.2 GHz is below which covers the overall band of UWB (3.1-10.6 GHz). The measured and simulated gain of the antenna along the Z-axis (φ=0° and θ=0°) are exhibited in Fig. 7 (b). With an average gain of 4.5dBi, the antenna has a maximum gain of 5.5 dBi over the UWB band. The slight deviation from the simulated curve is because of extended coaxial cable for feeding the antenna while measurement. Figure 8 shows the measured and simulated 2D and 3D normalized radiation pattern at 3.5, 6.5 and 9.5 GHz. Broadside radiation patterns are investigated for both the xz and yz plane. Here xz plane is acting as an Electric plane (E-plane) and yz plane is acting as a Magnetic plane (H-plane). In the E-plane, the patterns show the eight-shape-figure with some asymmetry for higher frequency. For H-plane cross-polarization radiation is higher than that of E-plane but still maintain the donut-shape with little distortion. It verifies that the antenna shows stable omnidirectional radiation pattern over the operating frequency. Due to fabrication and measurement tolerances, a little variation is observed in both E- and H-plane form simulated to the measured pattern.

Figure 9 (a) shows the antenna group delay. The group delay of face-to-face direction is more steady and lower than other two setup. It is because of the face to face direction most of the radiated power is received with minimum distortion. So, the prototype antenna will radiate efficiently towards the Region of Interest (ROI) while not coupling significantly with adjacent array elements. Furthermore, the group delay is linearly distributed over the frequency band.

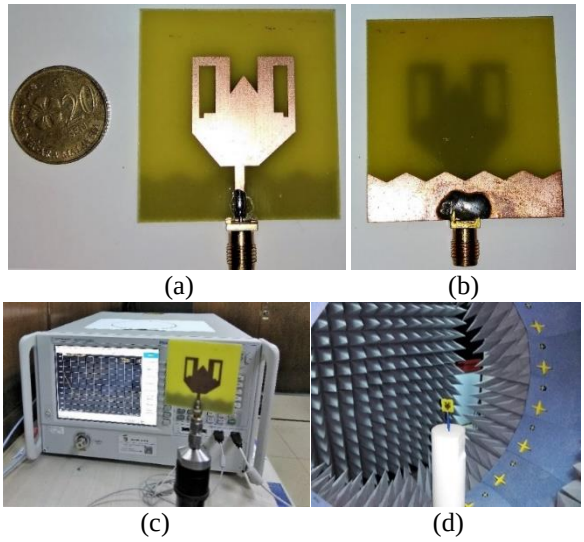

Fig. 6. Fabricated photograph of the prototype: (a) top view, (b) bottom view and measurement setup, (c) PNA network analyzer, and (d) Satimo Star Lab UKM.

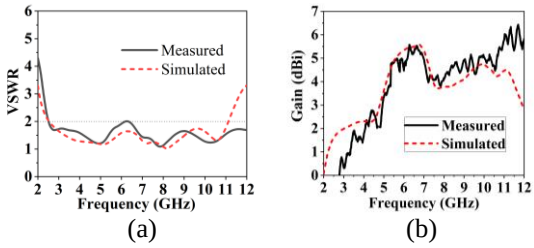

Fig. 7. Measured and simulated: (a) VSWR and (b) gain.

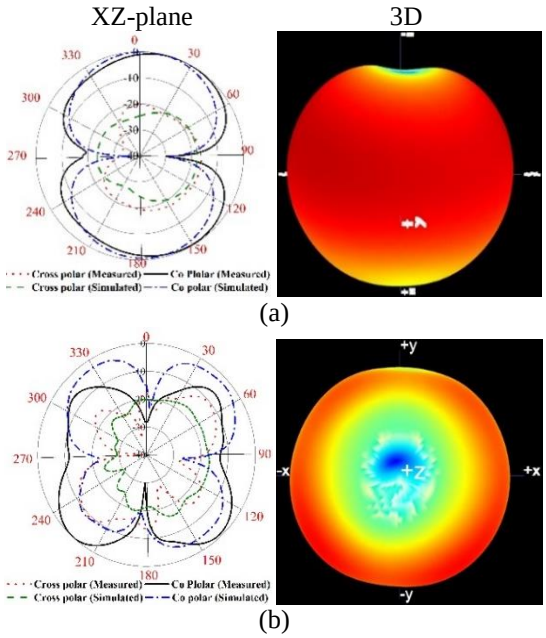

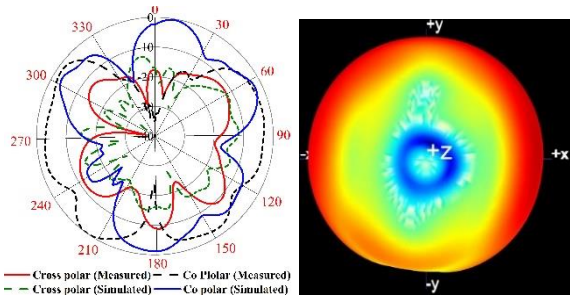

(c)

Fig. 8. 2D and 3D radiation pattern at: (a) 3.5 GHz, (b) 6.5 GHz, and (c) 9 GHz.

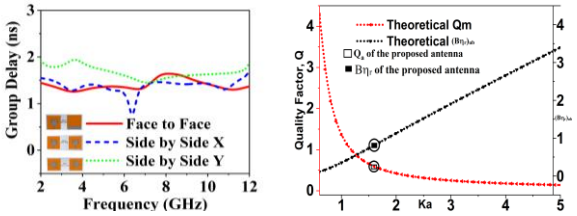

(a) (b)

Fig. 9. (a) Group delay for antenna positioned in face to face, side by side x and side by side y direction, and (b) theoretical limits and calculated Qa and (Bηr)ub.

Quality Factor:

With respect to the physical dimension of the antenna, minimum quality factor can be achieved by using the following equation [15]:

$$Q_{lb} = \eta Q . \tag{5}$$

Where $Q = \frac{1}{k^3 a^3} + \frac{1}{ka}$, $k = \frac{2\pi}{\lambda}$ and a denotes minimum sphere radius enclosed to the antenna. The higher bound of the radiation efficiency is:

$$(B\eta r)_{ub} = \frac{1}{\sqrt{2}} \left[\frac{1}{ka} + \frac{1}{k^3 a^3} \right]^{-1} . \tag{6}$$

The Q_m and $(B\eta r)_{ub}$ for different theoretical values of ka is shown in Fig. 9 (b). The antenna calculated value of ka=1.59 for the 1st resonant frequency. From the ideal curve it is noticed that the minimum limit of Q_m is 0.59 and $(B\eta r)_{ub}$ =0.81. The quality factor of the prototype is estimated through:

$$Q_a = \frac{2\sqrt{\beta}}{B}, \tag{7}$$

where, $\sqrt{\beta} = \frac{s-1}{2\sqrt{s}} \le 1$.

Here s=2 is considered as the maximum accepted VSWR. The achieved Q_a of the anticipated antenna is 0.56 and $(B\eta r)_{ub}$ =0.80 which indicates that the theoretical and calculated value is very close. This verifies that the antenna design is optimal.

C. Near field performance analysis

Since the dielectric properties can vary significantly between different patients, it is not reasonable to optimize the antenna in presence of a specific dielectric breast phantom. After optimization in free space, the authors checked the fidelity factor and near field directivity (NFD) to ensure that the near field radiation properties, like phase linearity, are maintained. The fidelity factors were investigated with the antennas in close proximity similar to the final imaging setup. The pattern of the output signal at receiving antenna depends on the input signal and transfer function. By performing the inverse Fourier transform, the transfer function can be turned to the time domain. Figures 10 (a-c) shows the time domain performance of the prototype for three different scenarios of face-to-face, side-by-side X and side-by-side Y at 300 mm distance. It is observed that the wave pattern is almost similar to the input and received signal for three cases which ensures that the antenna is able to transmit short pulses in minimum time and different directions with minimal distortion. Fidelity factor (FF) is critical [16, 17] to validate the correspondence between the transmitter (Tx) and received (Rx) signals. The highest value of cross-correlation between transmitting and receiving pulse is known as fidelity factor. Naturally, the pulse becomes almost distorted if an adjustment is higher than 50% (FF < 0.5) [16]:

$$F = \max \left(\frac{\int_{-\infty}^{+\infty} x(t)\, y(t-\tau)\, dt}{\sqrt{\int_{-\infty}^{+\infty} |x(t)^2| dt \int_{-\infty}^{+\infty} |y(t)^2| dt}} \right). \tag{8}$$

Where, x(t) and y(t) represents the T_X and R_X signals, respectively. For different scenario, the fidelity factor is 84%, 78% and 72% for face to face, side by side X and side by side Y respectively which indicates that the antennas transmitting and receiving capability are quite decent. The higher fidelity factor indicates the lower distortion and also suggests that this can be used for target detection. The phase distortion of the signal of an antenna is represented by group delay.

The NFD can be computed by using the formula presented in [18]. The NFD factor is the proportion of the power radiated inside the front side (Pf) and through the surface of the phantom (PT):

$$NFD = \frac{Pf}{PT} . \tag{9}$$

Figure 10 (d) illustrates the NFD of the proposed antenna with breast phantom. It is observed that about 67% of the total power is emitted through the ROI.

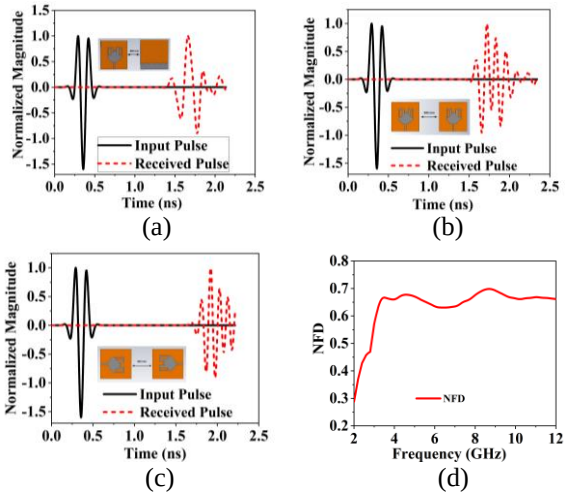

Fig. 10. The normalized magnitude of the proposed prototype for three different scenarios: (a) face to face, (b) side by side X, (c) side by side Y, and (d) NFD of the proposed antenna.

D. Imaging setup and results

The dielectric properties of the human breast are introduced in this section. A breast phantom is used to test the antenna array performance in detection of breast tumor. The phantom is constructed with four layers of skin, breast tissue, fat and regular air layer. The skin layer width is 2.5mm and dielectric constant is 38 with a conductivity of 1.49 S/m. The width of the breast tissue is 8.75 cm with a dielectric constant of 5.14 and 0.141 S/m of conductivity. The dielectric property of breast phantom is summarized in Table 2 [19]. An l imaging setup is proposed in this paper and shown in Fig. 11 (a). A heterogeneous breast phantom is used for characterization. The setup consists of 9 antenna unit placed vertically surrounding the breast phantom in every 40-degree interval from each other. The distance between the phantom and antenna array is 15mm. Frequency domain setup is applied to analyze the backscattering signal placing the antenna 1 as transmitter and rest of the antennas are acting as transmitter. By feeding the 1st antenna the effect of breast tissues is observed. Figure 11 (b) shows the Skin, Fat and Tumor dielectric constant vs frequency.

Table 2: The dielectric property of breast phantom

Tissue	ε′
Normal Tissue	38
Fat	5.14
Tumor (Malignant)	67

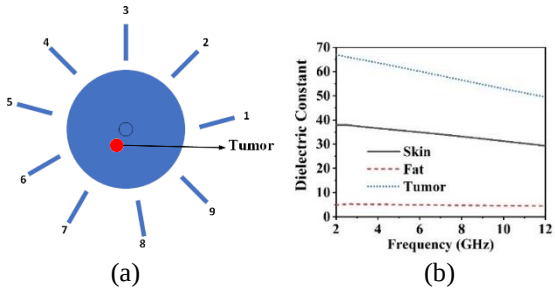

Fig. 11. Proposed model of breast phantom screening using: (a) 9-antenna unit; No. 1 is transmitting and another 8 are receiving the signal, and (b) skin, fat and tumor dielectric constant vs frequency.

Figure 12 represents the s-parameters of the proposed antenna array setup for two different scenarios. Figure 12 (a) represents the s parameters without the presence of tumor inside the phantom while antenna 1 is transmitting and another 8 antennas are receiving the scattered signals. Figure 12 (b) represents the backscattered signal of the system setup with the presence of tumor inside the breast phantom. There is a significant distortion of the backscattering signal of the two graphs. For the absence of tumor, the maximum of the reflection coefficient at the peak resonance frequency is recorded as -65dB while with tumor the peak is around -80dB. The scattered waveform is different because of the higher dielectric properties of the tumor comparing to the normal breast tissue. This indicates that our system can be a good candidate for microwave imaging to detect the unwanted cell like tumor through analyzing backscattering signal efficiently. A comparative study of reported antennas with proposed one is listed in Table 3. The considered parameters are bandwidth (BW), dimension, antenna gain, no of array elements and application. It is observed that the proposed antenna has compact dimension, good gain and wider bandwidth than the reports antennas.

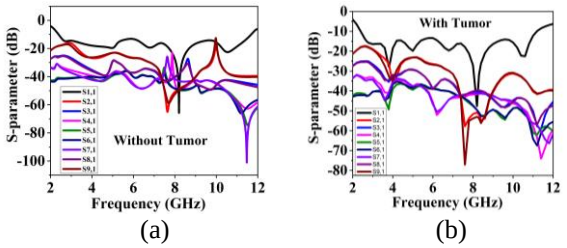

Fig. 12. S-parameter of the antenna array setup: (a) without the presence of tumor inside the phantom, and (b) with the presence of tumor inside the phantom.

Table 3: Comparison between the reported antenna and proposed antenna

Antennas	BW GHz (–10 dB)	Dimension Area (Single Element) (mm^2)	Gain (dBi)	Array Element	Applications
[4]	3.5–15	44 × 52.4	Not reported	4×4	Microwave Imaging
[7]	2.7–7	45 × 53	7.7	Single antenna	Microwave Imaging
[9]	3.5-18	38 × 40	4.5	Single antenna	Microwave Imaging
[13]	1.2–7	30 × 15	Not reported	16	Microwave Sensing
Proposed	2.5 – 11.2	44 × 42	5.5	9	Microwave Imaging

III. CONCLUSION

The design of a novel compact UWB antenna with excellent frequency ratio for microwave breast imaging for tumor detection with the electrical dimension of $0.367\lambda \times 0.350\lambda \times 0.013\lambda$ has been measured and categorized. The results show that the antenna has the fractional bandwidth of 127% (2.5 GHz to 11.2 GHz) with VSWR<2. The antenna has optimum design with good Q-factor value. The antenna has stable omnidirectional radiation pattern with peak gain of 5.5 dBi. The antenna also shows excellent time domain performance to be selected as suitable for microwave imaging. The NFD performance is also satisfactory. This compact and low-cost antenna is further used to design an array setup with a breast phantom to observe the behavior of the normal breast tissue and tumor cell by analyzing the received backscattering signals. The analysis of the signal shows that the tumor behaves different than normal breast tissue and this is the key point to identify the presence of tumor cell inside breast tissue. The antenna is a good candidate for early breast tumor detection through microwave imaging as it covers the UWB bandwidth with good performance in both time and frequency domain characteristics.

ACKNOWLEDGMENTS

This work was supported by the University Kebangsaan Malaysia, under GUP-2017-095 and MI-2017-001.

REFERENCES

[1] P. T. Huynh, A. M. Jarolimek, and S. Daye, "The false-negative mammogram," *Radiographics*, vol. 18, pp. 1137-1154, 1998.

[2] T. Henriksson, M. Klemm, D. Gibbins, J. Leendertz, T. Horseman, A. Preece, *et al.*, "Clinical trials of a multistatic UWB radar for breast imaging," in *Antennas and Propagation Conference (LAPC), 2011 Loughborough*, pp. 1-4, 2011.

[3] M. Bassi, M. Caruso, M. S. Khan, A. Bevilacqua, A.-D. Capobianco, and A. Neviani, "An integrated microwave imaging radar with planar antennas for breast cancer detection," *IEEE Transactions on Microwave Theory and Techniques*, vol. 61, pp. 2108-2118, 2013.

[4] T. Sugitani, S. Kubota, A. Toya, X. Xiao, and T. Kikkawa, "A compact 4x4 planar UWB antenna array for 3-D breast cancer detection," *IEEE Antennas and Wireless Propagation Letters*, vol. 12, pp. 733-736, 2013.

[5] M. Rokunuzzaman, M. Samsuzzaman, and M. T. Islam, "Unidirectional wideband 3-D antenna for human head-imaging application," *IEEE Antennas and Wireless Propagation Letters*, vol. 16, pp. 169-172, 2017.

[6] A. Afifi, A. Abdel-Rahman, A. Allam, and A. A. El-Hameed, "A compact ultra-wideband monopole antenna for breast cancer detection," in *Circuits and Systems (MWSCAS), 2016 IEEE 59th International Midwest Symposium on*, pp. 1-4, 2016.

[7] M. Z. Mahmud, M. T. Islam, M. N. Rahman, T. Alam, and M. Samsuzzaman, "A miniaturized directional antenna for microwave breast imaging applications," *International Journal of Microwave and Wireless Technologies*, vol. 9, pp. 2013-2018, 2017.

[8] W. Shao, A. Edalati, T. R. McCollough, and W. J. McCollough, "A time-domain measurement system for UWB microwave imaging," *IEEE Transactions on Microwave Theory and Techniques*, 2018.

[9] M. Kahar, A. Ray, D. Sarkar, and P. Sarkar, "An UWB microstrip monopole antenna for breast tumor detection," *Microwave and Optical Technology Letters*, vol. 57, pp. 49-54, 2015.

[10] T. Gholipur and M. Nakhkash, "Optimized matching liquid with wide-slot antenna for microwave breast imaging," *AEU-International Journal of Electronics and Communications*, 2018.

[11] M. Islam, M. T. Islam, M. R. I. Faruque, N. Misran, M. Samsuzzaman, M. Hossain, *et al.*, "A compact disc-shaped super wideband patch antenna with a structure of parasitic element," *International Journal of Applied Electromagnetics and Mechanics*, vol. 50, pp. 11-28, 2016.

[12] M. Mahmud, S. Kibria, M. Samsuzzaman, N. Misran, and M. Islam, "A new high performance hibiscus petal Pattern monopole antenna for UWB Aapplications," *Applied Computational Electromagnetics Society Journal*, vol. 31, 2016.

[13] M. Jalilvand, X. Li, L. Zwirello, and T. Zwick, "Ultra wideband compact near-field imaging system for breast cancer detection," *IET Microwaves*,

Antennas & Propagation, vol. 9, pp. 1009-1014, 2015.

[14] W. L. Stutzman and G. A. Thiele, *Antenna Theory and Design*. John Wiley & Sons, 2012.

[15] G. A. Mavridis, D. E. Anagnostou, and M. T. Chryssomallis, "Evaluation of the quality factor, q, of electrically small microstrip-patch antennas [wireless corner]," *IEEE Antennas and Propagation Magazine*, vol. 53, pp. 216-224, 2011.

[16] G. Quintero, J.-F. Zurcher, and A. K. Skrivervik, "System fidelity factor: A new method for comparing UWB antennas," *IEEE Transactions on Antennas and Propagation*, vol. 59, pp. 2502-2512, 2011.

[17] M. T. Islam, M. Samsuzzaman, M. Rahman, and M. Islam, "A compact slotted patch antenna for breast tumor detection," *Microwave Opt. Technol. Lett.*, vol. 60, pp. 1600-1608, 2018.

[18] R. K Amineh, A. Trehan, and N. K. Nikolova, "TEM horn antenna for ultra-wide band microwave breast imaging," *Progress In Electromagnetics Research*, vol. 13, pp. 59-74, 2009.

[19] S. Gabriel, R. Lau, and C. Gabriel, "The dielectric properties of biological tissues: II. Measurements in the frequency range 10 Hz to 20 GHz," *Physics in Medicine and Biology*, vol. 41, p. 2251, 1996.

Md. Tarikul Islam was born in Patuakhali, Bangladesh in 1994. He received his B.Sc. in Computer Science and Engineering from Patuakhali Science and Technology University (PSTU) in 2016. Currently he is working as a master's student in the Universiti Kebangsaan Malaysia (UKM), Malaysia. He has authored or co-authored a number referred journals and conference papers. He is currently a Graduate Research Assistant at the Department of Electrical, Electronic and Systems Engineering, UKM, Malaysia. His research interests include the communication antenna design, Wireless Communication, RF Engineering and Microwave Imaging.

Md. Samsuzzaman was born in Jhenaidah, Bangladesh in 1982. He received his B.Sc. and M.Sc. degrees in Computer Science and Engineering from the Islamic University Kushtia, Bangladesh in 2005 and 2007, respectively, and the Ph.D. degree from the Universiti Kebangsaan Malaysia, Malaysia 2015. From February 2008 to February 2011, he worked as a Lecturer at the Patuakhali Science and Technology University (PSTU), Bangladesh. From February 2011 to 2015, he worked as an Assistant Professor at the same university. He is now working as a Post-doctoral Fellow at the Universiti Kebangsaan Malaysia. He has authored or co-authored approximately 100 referred journals and conference papers. His research interests include the communication antenna design, satellite antennas, and satellite communication.

Iskandar Yahya is a Senior Lecturer at the Centre of Advanced Electronic and Communication Engineering (PAKET), Faculty of Engineering and Built Environment, Universiti Kebangsaan Malaysia (UKM). He is also an Associate Research Fellow at the Institute of Microengineering and Nanoelectronics (IMEN) in UKM. He obtained his Master of Engineering (M.Eng.) in Electrical & Electronic Engineering (Communications) from The University of Sheffield in 2006. He later joined the Advanced Technology Institute, University of Surrey as a post-graduate and in 2013 obtained his Ph.D. in Electronics Engineering. His research interests include semi-conductor devices, nanoelectronics devices, carbon-based electronics and advanced materials for electro-magnetic propagation devices. He is currently teaching undergraduate electrical and electronic engineering courses for the electrical and electronic engineering program in UKM.

Mohammad Tariqul Islam is a Professor at the Department of Electrical, Electronic and Systems Engineering of the Universiti Kebangsaan Malaysia (UKM) and visiting Professor of Kyushu Institute of Technology, Japan. He is the author and co-author of about 350 research journal articles, nearly 165 conference articles, and a few book chapters on various topics related to antennas, microwaves and electromagnetic radiation analysis with 16 inventory patents filed. Thus far, his publications have been cited 3709 times and his H-index is 33 (Source: Scopus). His Google scholar citation is 5200 and H-index is 36. He is the recipient of more than 40 research grants from the Malaysian Ministry of Science, Technology and Innovation, Ministry of Education, UKM research grant, international research grants from Japan and Saudi Arabia. His research interests include communication antenna design, radio astronomy antennas, satellite antennas, and electromagnetic radiation analysis. Islam currently serves as the Editor-in-Chief for the International Journal of Electronics and Informatics and Associate Editor for Electronics Letter. He received several International Gold

Medal Awards, a Best Invention in Telecommunication Award, a Special Award from Vietnam for his research and innovation, and Best Researcher Awards in 2010 and 2011 at UKM. He also won the Best Innovation Award in 2011 and the Best Research Group in ICT Niche in 2014 by UKM. He was the recipient of Publication Award from Malaysian Space Agency in 2014, 2013, 2010, 2009 and the Best Paper Presentation Award in 2012 International Symposium on Antennas and Propagation, (ISAP 2012) at Nagoya, Japan and in 2015 in IconSpace. He is a Senior Member of IEEE, Chartered Professional Engineer-CEng, Member of IET (UK) and member of IEICE (Japan).